

# Design and Application of Lattice Structures on Sandwich Panels Core

José Guilherme Fonseca Clemente Monteiro

zeguilherme.monteiro@gmail.com

Instituto Superior Técnico, University of Lisbon, Portugal

November 2019

## Abstract

Sandwich panels with truss cores represent an alternative to honeycomb core design, as they are structures that lead to high stiffness, strength and energy absorption with low weight. The main purpose of this research is to investigate the effect of the lattice topology on the flexural behaviour of the sandwich panels. Five lattice geometries were studied, namely body centred (BC), body centred with struts in z-axis (BCZ), body face centred with struts in z-axis (BFCZ), face centred with struts in z-axis (FCZ) and parallelepipedic simple (PS). The relative density was kept the same for all the lattices considered as 0.3, which is one of the commonly used values of regular hexagonal honeycombs. Both numerical and experimental approaches were used to evaluate the flexural properties of the composite structures in a three-point bending test. The numerical analysis was undertaken with the finite element software, Siemens NX. Fused deposition modelling (FDM) was used to print polylactic acid samples with the configurations listed. The sandwich samples are composed of a lattice core and two thin plates, at the bottom and top, which were manufactured all together. FDM specimens were experimentally tested to evaluate the mechanical response and the failure behaviour of the cores. Among the lattices experimentally studied, lattice BCZ exhibits the higher strength, while BC shows higher stiffness and BFCZ achieves the highest energy absorption. The higher values obtained by these lattices are close to the ones obtained with a cellular two-dimensional hexagonal structure with the same relative density. Consequently, some of the structures studied may be alternatives to conventional structures in the design process of composite materials.

**Keywords:** Sandwich panels, lattice structures, fused deposition modelling, three-point bending, numerical simulations

## 1. Introduction

One of the main objectives in structural design is to attain the lightest possible load-carrying capability with high stiffness and strength. Sandwich structures satisfy these assumptions due to their low relative density, high strength, high energy absorption and relevant bending stiffness (Figure 1).

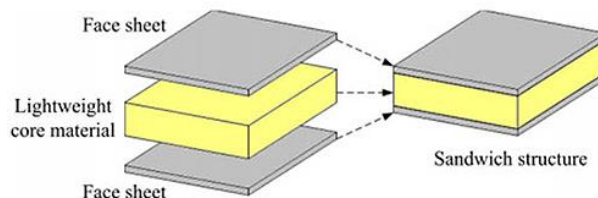


Figure 1: Components of a sandwich structure [1].

Lattice structures are defined in literature as periodic structures, continuously repeating unit cells that inter-connect each other in three dimensions. They are typically created from truss structures, as well as minimalistic surfaces. While 3D cellular solids or foams are random structures due to the

manufacturing process, to fabricate this kind of structures AM methods come up in front as it allows an increased geometrical design freedom and a good range of potential materials to be used. AM lattices are popular because they exhibit various advantages over solid structures and non-additively manufactured cellular solids. They have all the advantages of cellular solids, for example, low-mass and high impact energy absorption, and have the additional advantage of design freedom that permit topologically optimized solutions to various problems, for instance, vibration isolation [2]. Recently, several researchers have investigated the influence of input parameters on lattice structures under compressive and bending strength [3, 4, 5]. Some authors have studied the dependency of their constituent material, geometrical parameters and core cell topology on their structural and energy absorption performance as well as in their failure mechanisms. Also it was studied the impact of bio-based tissue engineered scaffolds for medicinal use [5, 6]. Others have studied the impact of the unit cell on the deformation behaviour of cellular structures. According with Linul et al. [7] the unit cell shape design is an effective way to control the mechanical properties of the reticulate meshes such as the elastic modulus, compressive strength and deformation behaviour. Although there is abundant published work about the behaviour of specific types of individual lattice structures, only a few have been made to compare the mechanical response and energy absorption characteristic of 3D printed lattices of different types of unit cells made of identical relative density [8]. Following works, that have been developed in Lab2ProD, regarding fabrication and analysis of 2D core sandwich structures it has arisen the idea to study the new-found 3D lattices core sandwich structures. The objective of this document is to design, produce and analyse the stiffness, strength and energy absorption of six sandwich panels, differing in core geometry. Five geometries were developed using lattices and a sixth honeycomb type structure was used as benchmark for the study. All of them with the same core relative density. To accomplish this, the following steps were to be achieved: design six-unit cell beam structures (panels) all with core relative density of 0,30 and approximately similar global dimensions; carry out a FEA in each one of the sandwich panels subjected to a three-point bending loading; produce all the sandwich panels using FDM process in a comercial 3D printing machine; experimental testing of all the six panels subjected to a three-point bending loading; compare the five lattice structures in terms of load-displacement curves, rigidity and absorbed energy with the benchmark honeycomb structure; compare the results of FEA with the experimental tests.

## 2. Materials and Methods

A material named poly-lactic acid (PLA) was used for the design of the specimens. It is a thermoplastic polymer (aliphatic polyester) derived from renewable biomass, commonly from fermented plant starch. Known for its high-modulus and high-strength, PLA is also biodegradable (degrade into innocuous lactic acid), therefore it is used in many fields of applications, from food packaging to medical prostheses.

### 2.1. Specimens Design

In total, eighteen models (three for each of the six topologies) were made using CAD software Solidworks 2018. The specimens were created with approximately the same global dimensions - Length (L), Width (W) and Total thickness (T) - and core relative density ( $\rho_c$ ), all present in Table 1.

Table 1: Approximate global dimensions and core relative density of the specimens.

Property	Amount
Length (mm)	167
Width (mm)	53
Total Thickness (mm)	22
Core relative density (-)	0.3

The six configurations consist of five lattice structures identified by: Body Centred (BC), Body Centred with Z axis struts (BCZ), Body and Face Centred with Z axis struts (BFCZ), Face Centred with Z axis struts (FCZ) and Parallelepipedic Simple (PS) (Figure 2). A honeycomb structure, the hexagonal honeycomb was also studied (Figure 3).

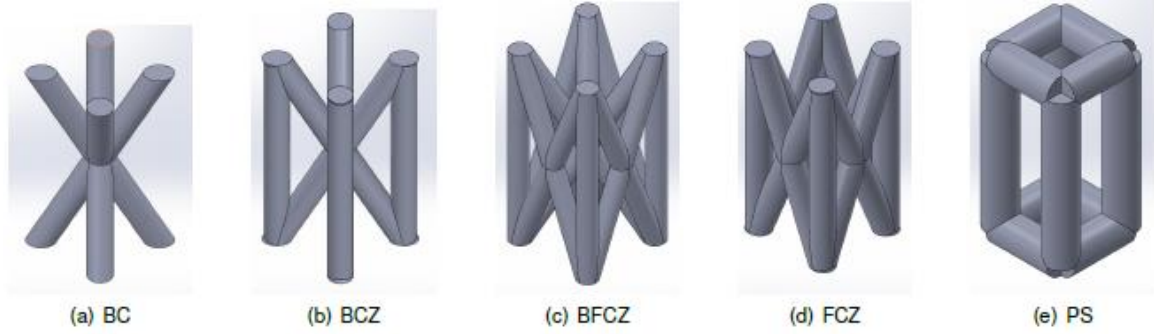


Figure 2: Lattice unit cells analysed in this document.

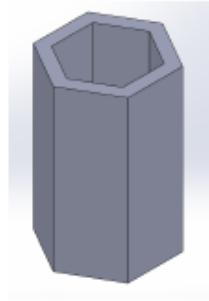


Figure 3: Hexagonal honeycomb unit cell.

The relative density of the arrangements depends on the parameters  $r$  for the strut radius of the lattice structures and  $l$  and  $t_0$  for the length and wall thickness of the honeycomb one. Due to the printer resolution, it is not physically possible to obtain the same relative density for all of them, although a good approximate value is possible to attain. After computing the variable parameters related to the struts radius ( $r$ ), honeycomb cell length ( $l$ ) and wall thickness ( $t_0$ ) together with the occupied core volume ( $V_0$ ) were obtained the variables  $r$ ,  $l$  and  $t_0$  as can be seen in Tables 2 and 3. This procedure made possible to build the final models with same core relative density.

Table 2: Variable parameter  $r$  of lattice structures with fixed L, W, T and  $\rho_c$ .

Lattice Structures	$r$ (mm)
BC	1.35
BCZ	1.19
BFCZ	0.92
FCZ	1.23
PS	1.90

Table 3: Variable parameters  $l$  and  $t_0$  of honeycomb structure with fixed L, W, T and  $\rho_c$ .

Honeycomb Structure	$l$ (mm)	$t_0$ (mm)
HEX	5	1.4

It can be observed from Table 2 that the unit cells that have more components have their struts' diameter thinner in order to keep the relative density constant. In terms of cell dimensions were defined two different categories: one for the lattice structures and other to the honeycomb one. It was defined a unit cell implantation section dimension for the lattices of  $8.166 \times 8.166 \text{ mm}^2$  and  $10.06 \times 10.06 \text{ mm}^2$  for the hexagonal honeycomb. Multiplying the cellular dimensions of 20 in length by 6 in width one arrives to the final pattern of the lattice structures. On the other hand, making the multiplication of 21 in length by 8 in width it is possible to arrive to the final pattern of the honeycomb specimen.

## 2.2. Specimens manufacture

The specimens were manufactured through FDM technology using a Ultimaker 3 machine with an infill fraction of 100% and without the use of supports, as seen in Figure 4. The model is firstly generated in a CAD program and then exported as an STL file. Then, the Slicer software, in this case CURA from Ultimaker, slices the models into layers and generates the G-code meant to be interpreted by the machine.

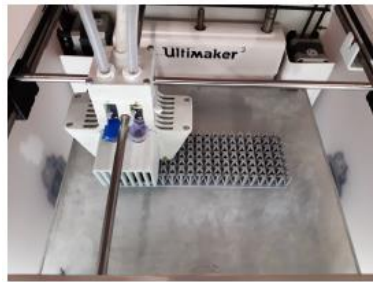


Figure 4: Ultimaker 3 3D printer present in Lab2ProD during manufacture.

Although, some minor defects can be seen in all the specimens, for example, stringing and minor layer shifts, these were considered as non-compromising for the study.

## 2.3. Experimental procedure

For each of the six geometries three samples were fabricated to perform 3PB tests. In Figure 5 all the samples printed by FDM for each core geometry are exhibited.



Figure 5: Groups of three equal samples before 3PB test.

Before making the tests, the dimensions and weight of the specimens were measured and are summarized in Table 4.

Table 4: Dimensions, densities and weight of tested specimens.

Topology	W (mm)	L (mm)	T (mm)	$\rho_c$	$\rho_{total}$	w (g)
BC_1	167	53	22	0.296	0.38	86
BC_2	167	53	22	0.296	0.38	86
BC_3	167	53	22	0.292	0.38	85
BCZ_1	167	53	22	0.292	0.38	85
BCZ_2	167	53	22	0.296	0.38	86
BCZ_3	167	53	22	0.296	0.38	86
BFCZ_1	167	53	22	0.296	0.38	86
BFCZ_2	167	53	22	0.296	0.38	86
BFCZ_3	167	53	22	0.306	0.38	88
FCZ_1	167	53	22	0.292	0.38	85
FCZ_2	167	53	22	0.296	0.38	86
FCZ_3	167	53	22	0.292	0.38	85
PS_1	167	53	22	0.292	0.38	85
PS_2	167	53	22	0.296	0.38	86
PS_3	167	53	22	0.296	0.38	86
HEX_1	171	52	22	0.292	0.37	85
HEX_2	171	52	22	0.292	0.37	85
HEX_3	171	52	22	0.287	0.37	84

The 3PB test was performed following the standard ASTM C393 – 00 (Standard Test Method for Flexural Properties of Sandwich Constructions) [9]. Figure 6 exhibits a scheme of the three-point bending test where  $P_1$  is the applied load and  $L_1$  is the support span which was around 117 mm for all tests.

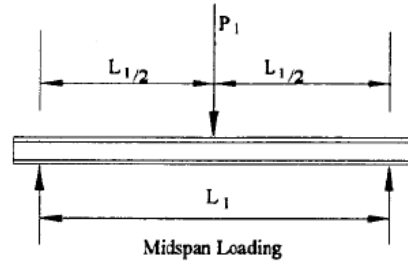


Figure 6: Loading diagram.

Figure 7 shows the set-up for the mechanical testing. In this particular case it is displayed the BFCZ\_1 specimen.

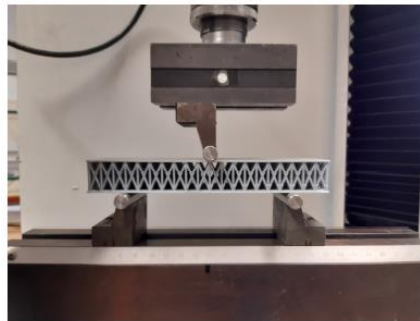


Figure 7: Experimental set-up for 3PB test.

The equipment Instron 3369 was used during all experimental process, Figure 8 shows the apparatus of the machine which has a load cell of 50 kN. For all tests, a 2.5 mm/min crosshead speed for the upper roller was defined. The load-displacement curves from the test were obtained with the Bluehill software.

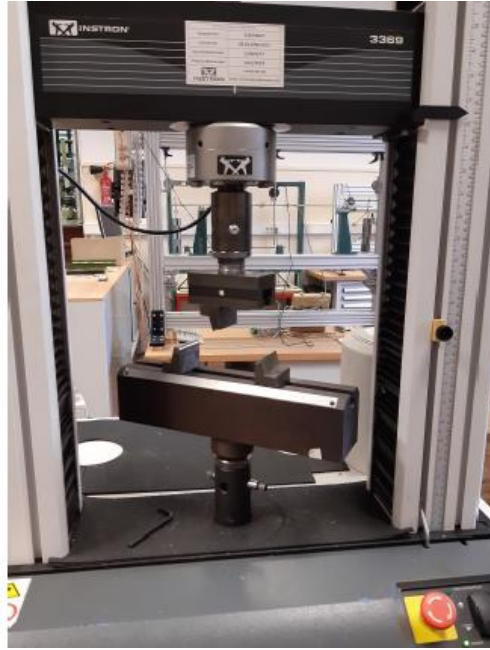


Figure 8: Instron 3369 equipment.

## 2.4. Numerical simulation

For the numerical simulations it was used the software Siemens NX, version 18.51.2602. The program uses finite element method (FEM) to do its calculations. The Siemens NX online guide [10] was fundamental to the implementation of FEA. For the complete analysis process, in all configurations, the programme needs three types of files: part, fem and sim (Figure 9). In the end, a solution solver was used.

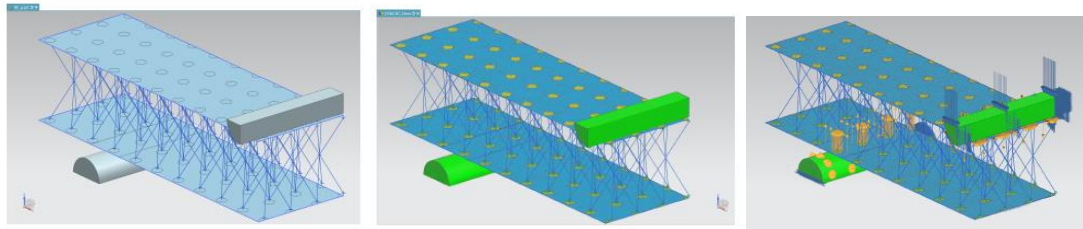


Figure 9: BC part, fem and sim files made in Siemens NX software.

Mesh convergence studies were performed with a certain criteria to guarantee an improvement in the accuracy of stress values without a large increase in the computational time. The convergence criterium was defined as less than 5% changes in the maximum von Mises stress.

## 3. Results and Discussion

### 3.1. Numerical simulations

The numerical simulation is based in a linear elastic analysis made in Siemens NX. In Figure 10 it is shown the illustrative results of the FEA of all the lattice structures analyzed (BC, BCZ, BFCZ, FCZ and PS, per order of appearance) and of the hexagonal honeycomb structure. In particular, it is displayed the elemental von Mises stresses in the skins.

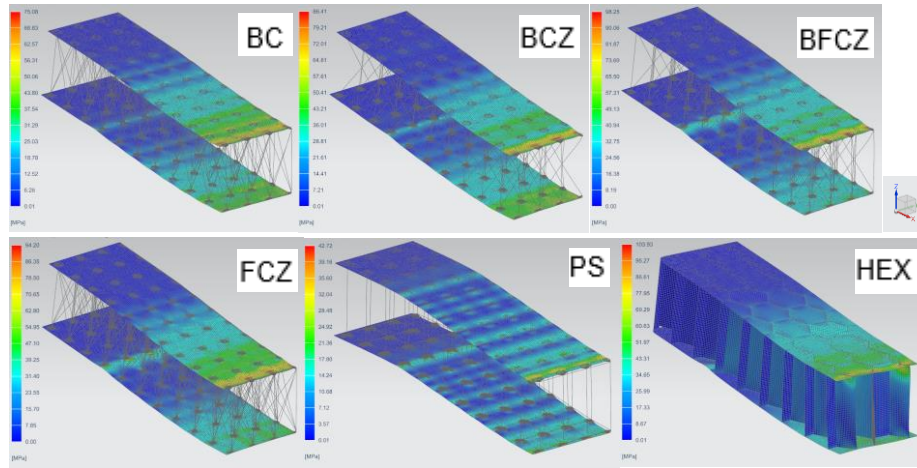


Figure 10: Elemental von Mises stress in the skins of all the structures under 3PB loading

Figure 11 shows all the load-displacement linear curves from the numerical analysis. With them it is possible to set reference values for maximum load, stiffness  $K$  and absorbed energy (Table 5) that will be used to compare with experimental results. Maximum load was defined to be the load for an input vertical displacement of 4 mm, stiffness  $K$  is the slope of the linear load-displacement curve and the absorbed energy is attained by calculating the area below the curve.

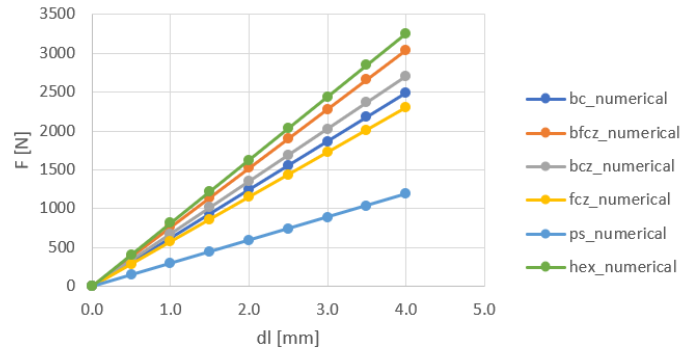


Figure 11: Load-displacement numerical curves of all topologies analysed in this document.

In Table 5 one can see the differences between the maximum load (strength), stiffness  $K$ , absorbed energy and von Mises stress of the different topologies. The lattice structure that comes closer to the honeycomb is BFCZ. However, BCZ has a closer von Mises stress in comparison with the hexagonal honeycomb.

Table 5: Maximum load, stiffness, energy absorption and maximum von Mises stress for all the topologies.

Topology	$\rho_c$ (-)	Maximum load (N)	Stiffness $K$ (N/mm)	Energy absorption (J)	Max $\sigma_{vM}$ (MPa)
BC	0.3	2490	622	4.98	86.39
BCZ	0.3	2702	676	5.40	98.25
BFCZ	0.3	3042	760	6.08	94.20
FCZ	0.3	2300	575	4.60	75.08
PS	0.3	1187	297	2.37	42.73
HEX	0.3	3249	812	6.50	103.93

### 3.2. Experimental tests

From the load-displacement curves the initial stiffness (the slope of the linear region) and the energy absorbed until maximum load were calculated for all the specimens and are displayed in Table 6.

Experimentally, the stiffness is higher for BC structures and the energy absorbed is higher for BFCZ structures. In Figure 12 one can see all the failed specimens after the 3PB test.

Table 6: Rupture displacement, maximum load, stiffness K and energy absorption of all the topologies

Topology	$\rho_c$ (-)	dl rupture (mm)	Maximum load (N)	Stiffness $K$ (N/mm)	Energy absorption (J)
BC_1	0.3	3.43	2806	1096	6.09
BC_2	0.3	3.23	2780	1106	5.69
BC_3	0.3	3.20	2755	1091	5.12
BC_average	0.3	$3.29 \pm 0.10$	$2780 \pm 21$	$1098 \pm 6$	$5.63 \pm 0.40$
BCZ_1	0.3	3.80	2796	1024	6.55
BCZ_2	0.3	3.67	2795	1049	6.29
BCZ_3	0.3	3.65	2807	1049	6.26
BCZ_average	0.3	$3.71 \pm 0.07$	$2799 \pm 5$	$1041 \pm 12$	$6.37 \pm 0.13$
BFCZ_1	0.3	3.84	2713	991	6.47
BFCZ_2	0.3	3.48	2632	952	6.07
BFCZ_3	0.3	3.75	2796	1030	6.64
BFCZ_average	0.3	$3.69 \pm 0.15$	$2714 \pm 67$	$991 \pm 32$	$6.39 \pm 0.24$
FCZ_1	0.3	3.55	2656	935	5.29
FCZ_2	0.3	3.87	2749	946	6.40
FCZ_3	0.3	3.63	2853	957	6.05
FCZ_average	0.3	$3.68 \pm 0.14$	$2753 \pm 80$	$946 \pm 9$	$5.91 \pm 0.46$
PS_1	0.3	2.85	1212	487	3.11
PS_2	0.3	2.64	1214	516	3.20
PS_3	0.3	2.82	1187	465	2.96
PS_average	0.3	$2.77 \pm 0.09$	$1204 \pm 12$	$489 \pm 21$	$3.09 \pm 0.10$
HEX_1	0.3	3.47	3752	1343	7.33
HEX_2	0.3	3.42	3738	1342	7.30
HEX_3	0.3	3.58	3790	1327	7.74
HEX_average	0.3	$3.49 \pm 0.07$	$3760 \pm 22$	$1337 \pm 7$	$7.46 \pm 0.20$

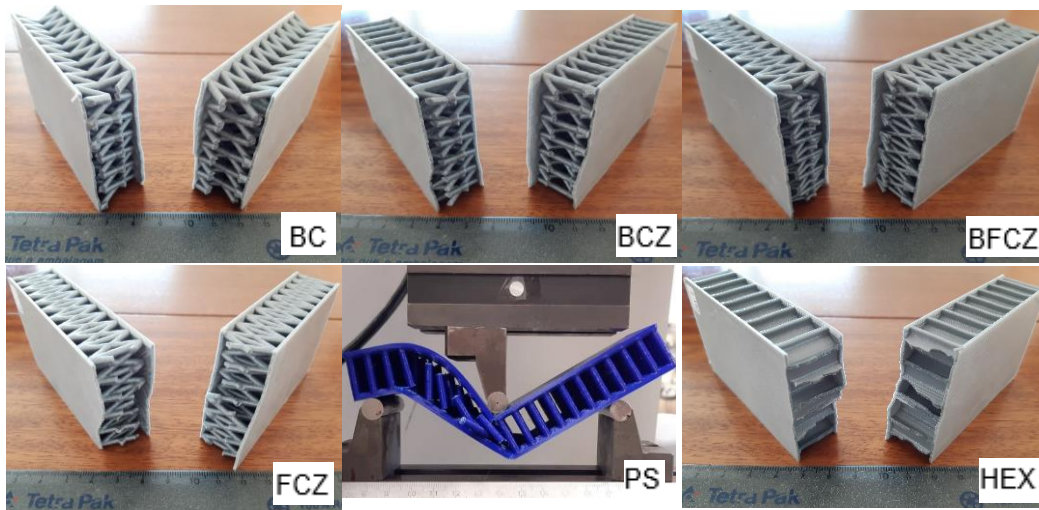


Figure 12: Broken specimens after 3PB test.

Two major theories were used to characterize the results obtained in this work: the unit cell mechanical behaviours of foams and lattices [3] (where the author explain the differences between bending and stretch dominated structures) and the failure mechanisms of lattice structures on sandwich beams [11] (where the authors define analytical formulae for the collapse strengths of each of the failure mechanisms of a specimen under 3PB). Unit cells struts are subjected to both bending and stretching in addition to other effects such as shearing, torsion and nodal interactions, however, one can observe that the lattice structures with diagonal struts (BC, BCZ, BFCZ and FCZ) have a bending dominated

behaviour in the fracture while the PS structure, because of the non-existence of diagonal struts in its constitution shows a stretching dominated behaviour. Accordingly with the failure mechanisms theory of sandwich structures, the majority fails by top face collapse, while PS fails by core shear.

### 3.3. Comparison between methods

Judging by the fracture surfaces in all specimens and considering the small plastic section in the experimental load-displacement curves of all the specimens, except for PS, one can say that brittle fractures are present. In Figure 13 are exhibited, as an example of the lattices structures, the experimental and numerical load-displacement curves of BFCZ topology documented in this work. For the PS topology it was only made a comparison for the initial linear elastic region (Figure 14).

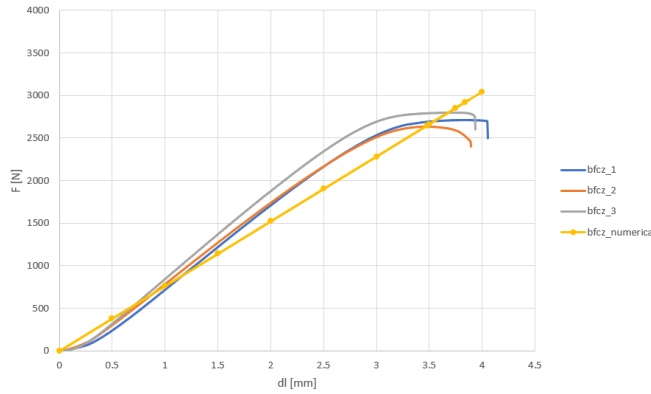


Figure 13: Load-displacement experimental and numerical curves of BFCZ topology.

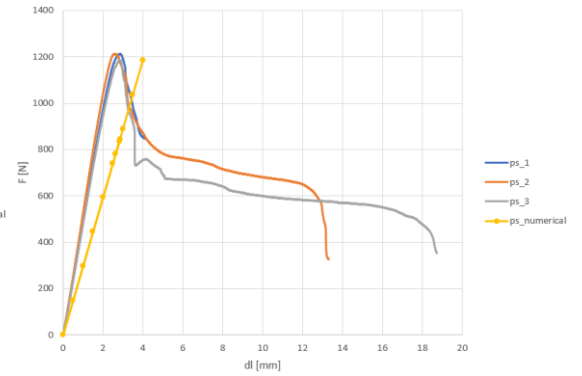


Figure 14: Load-displacement experimental and numerical curves of PS topology.

Applied load, stiffness and energy absorption are the main parameters studied in this thesis and these results are displayed in Table 7. There, it is seen a satisfactory agreement between experimental and FEA values. The results confirm that the hexagonal honeycomb structure is still ahead of the tested lattices, when comparing maximum supported load. Even so, when considering energy absorption and stiffness, the well-established honeycomb can be challenged. The higher experimental values of applied load and stiffness of lattices seen in Table 7 are the result of lattices with less struts where there is an increased influence of struts intersections at the nodes because of the higher value of contact area.

Table 7: Rupture displacement, maximum load, stiffness K and energy absorption of all the topologies for both experimental and numerical 3PB tests. (Average values for experimental tests and unique values for numerical simulations).

Topology	$\rho_c$ (-)	dl R (mm)	Load_num (N)	Load_exp (N)	K_num (N/mm)	K_exp (N/mm)	E abs_num (J)	E abs_exp (J)
BC	0.3	3.29	2046	2780	622	1098	4.98	5.63
BCZ	0.3	3.71	2504	2799	676	1041	5.40	6.37
BFCZ	0.3	3.69	2806	2714	760	991	6.08	6.39
FCZ	0.3	3.68	2116	2753	575	946	4.60	5.91
PS	0.3	2.77	822	1204	297	489	2.37	3.09
HEX	0.3	3.49	2835	3760	812	1337	6.50	7.46

Finally, one can see that the failure in all specimens happens in the top skin contact area with the moving roller which is concordant with the area of higher von Mises stress in FEA. In addition, it is also seen in the bending dominated lattices (BC, BCZ, BFCZ and FCZ) that the core failure appears in the top struts present in the middle span plane in connection with the top skin. This is coherent with the struts' maximum values of both shear and axial loads given by the numerical simulations.

## 4. Conclusions and future work

In this thesis five new lattice structures inspired in crystalline structures of atoms with cubic arrangements were designed to apply on sandwich panels core. These 3D composite panels were then compared to a commonly used 2D hexagonal honeycomb panel maintaining a constant core density in all tested specimens. Experimental tests and numerical simulations were used to analyze the mechanical response and the failure behaviour of all the cores through a three-point bending loading. Generally, a satisfactory agreement was found between FEA results and experimental results. Thus, it is seen that the failure in all specimens happens in the top skin area in contact with the moving roller which is concordant with the area of higher von Mises stress in FEA. As the relative density was kept constant, the main influencer of mechanical properties was the core geometry with body and faced centred topologies (BC, BCZ, BFCZ and FCZ) showing higher strength, stiffness and energy absorption than the parallelepipedic simple (PS) core panel. It is also visually and graphically observed in the samples that the BC, BCZ, BFCZ and FCZ core panels have bending dominated fractures behaviours, while PS core panel has a stretching dominated fracture behaviour. Finally, this work concludes that the higher values obtained by these lattices in terms of stiffness and energy absorption are close to the ones obtained with a cellular two-dimensional hexagonal structure with the same relative density. Therefore, lattices may be alternatives to conventional structures in the design of composite panels. Future work on this topic will consist of finding new lattices topologies that may overpass the flexural properties of the conventional hexagonal honeycomb structure. Topology optimization and generative design methods could be used as an alternative and concurrently with the methodologies approached in this work. Additionally, new core geometries can be developed with the increment of design freedom allowable by additive manufacturing. In the search for even more efficient lattice cores, future work should evaluate the influence of length/diameter ratio (slenderness) and of the manufacturing process in the mechanical response of the lattices.

## Acknowledgements

This work was supported by Fundação para a Ciência e Tecnologia (FCT), through IDMEC, under LAETA project, UID/EMS/50022/2019. The author gratefully acknowledges the funding of the BigFDM project, FCT Reference PTDC/EME-EME/32103/2017. The author also thanks Professor Fátima Vaz and Engineer Manuel Sardinha.

## References

- [1] TotalMateria. "sandwich steel panels: Part one". in: Total Materia website (2017). <https://www.totalmateria.com/page.aspx?ID=CheckArticle&site=kts&NM=484>. Accessed: 2019-09-13.
- [2] W. P. Syam, W. Jianwei, B. Zhao, I. Maskery, W. Elmadih, and R. Leach. Design and analysis of strut-based lattice structures for vibration isolation. *Precision Engineering*, 52(May 2017):494–506, 2018. doi: 10.1016/j.precisioneng.2017.09.010.
- [3] M. F. Ashby. The properties of foams and lattices. *Philosophical Transactions of the Royal Society of London Series a-Mathematical Physical and Engineering Sciences*, (364): pages 15–30, 2006. doi:10.1098/rsta.2005.1678.
- [4] H. Yazdani Sarvestani, A. H. Akbarzadeh, A. Mirbolghasemi, and K. Hermenean. 3D printed metasandwich structures: Failure mechanism, energy absorption and multi-hit capability. *Materials and Design*, 160:179–193, 2018. doi: 10.1016/j.matdes.2018.08.061.
- [5] F. N. Habib, M. Nikzad, S. H. Masood, and A. B. M. Saifullah. Design and Development of Scaffolds for Tissue Engineering Using Three-Dimensional Printing for Bio-Based Applications. *3D Printing and Additive Manufacturing*, 3(2):119–127, 2016. doi: 10.1089/3dp.2015.0014.
- [6] A. Kantaros, N. Chatzidai, and D. Karalekas. 3D printing-assisted design of scaffold structures. *Advanced Manufacturing Technology* 2015. doi: 10.1007/s00170-015-7386-6.
- [7] E. Linul, D. A. Serban, T. Voiconi, L. Marsavina, and T. Sadowski. Energy – absorption and efficiency diagrams of rigid PUR foams. *Key Engineering Materials*, 601:246–249, 2014. doi: 10.4028/www.scientific.net/KEM.601.246.
- [8] F. N. Habib, P. Iovenitti, S. H. Masood, and M. Nikzad. Fabrication of polymeric lattice structures for optimum energy absorption using Multi Jet Fusion technology. *Materials and Design*, 155(2017): 86–98, 2018. doi: 10.1016/j.matdes.2018.05.059.
- [9] ASTM C393-00. Standard Test Method for Flexural Properties of Sandwich Constructions. Standard, ASTM International, West Conshohocken, PA, Mar. 2000.
- [10] Siemens. "siemens nx online guide". in: Siemens website (2019). [https://docs.plm.automation.siemens.com/tdoc/nx/12/nx\\_help/#uid:index](https://docs.plm.automation.siemens.com/tdoc/nx/12/nx_help/#uid:index). Accessed: may-september 2019.
- [11] V. S. Deshpande and N. A. Fleck. Collapse of truss core sandwich beams in 3-point bending. *International Journal of Solids and Structures*, 38: 6275–6305, 2001.